oxLDL and eLDL Induced Membrane Microdomains in Human Macrophages

Stefan Wallner[1], Margot Grandl[1¤a], Gerhard Liebisch[1], Markus Peer[1¤b], Evelyn Orsó[1], Alexander Sigrüner[1], Andrzej Sobota[2], Gerd Schmitz[1]*

1 Institute for Clinical Chemistry and Laboratory Medicine, University Hospital Regensburg, Regensburg, Germany, 2 Department of Cell Biology, Nencki Institute of Experimental Biology, Warsaw, Poland

¤a Current address: Beckman-Coulter GmbH, Berlin, Germany
¤b Current address: Bruker Daltonics, Bremen, Germany
* gerd.schmitz@klinik.uni-regensburg.de

Abstract

Background

Extravasation of macrophages and formation of lipid-laden foam cells are key events in the development and progression of atherosclerosis. The degradation of atherogenic lipoproteins subsequently leads to alterations in cellular lipid metabolism that influence inflammatory signaling. Especially sphingolipids and ceramides are known to be involved in these processes. We therefore analyzed monocyte derived macrophages during differentiation and after loading with enzymatically (eLDL) and oxidatively (oxLDL) modified low-density lipoproteins (LDL).

Methods

Primary human monocytes were isolated from healthy, normolipidemic blood donors using leukapheresis and counterflow elutriation. On the fourth day of MCSF-induced differentiation eLDL (40 μg/ml) or oxLDL (80 μg/ml) were added for 48h. Lipid species were analyzed by quantitative tandem mass spectrometry. Taqman qPCR was performed to investigate transcriptional changes in enzymes involved in sphingolipid metabolism. Furthermore, membrane lipids were studied using flow cytometry and confocal microscopy.

Results

MCSF dependent phagocytic differentiation of blood monocytes had only minor effects on the sphingolipid composition. Levels of total sphingomyelin and total ceramide remained unchanged, while lactosylceramides, cholesterylesters and free cholesterol decreased. At the species level most ceramide species showed a reduction upon phagocytic differentiation. Loading with eLDL preferentially increased cellular cholesterol while loading with oxLDL increased cellular ceramide content. Activation of the salvage pathway with a higher mRNA expression of acid and neutral sphingomyelinase, neutral sphingomyelinase activation associated factor and glucosylceramidase as well as increased surface expression of SMPD1 were identified as potentially underlying mechanisms. Moreover, flow-cytometric analysis revealed a higher cell-surface-expression of ceramide, lactosylceramide (CDw17),

globotriaosylceramide (CD77), dodecasaccharide-ceramide (CD65s) and GM1 ganglioside
upon oxLDL loading. ApoE in contrast to apoA-I preferentially bound to the ceramide
enriched surfaces of oxLDL loaded cells. Confocal microscopy showed a co-localization of
acid sphingomyelinase with ceramide rich membrane microdomains.

Conclusion

eLDL leads to the formation of lipid droplets and preferentially induces cholesterol/sphingo-
myelin rich membrane microdomains while oxLDL promotes the development of choles-
terol/ceramide rich microdomains via activation of the salvage pathway.

Introduction

Atherosclerosis represents a leading cause of death in industrialized countries [1, 2]. It is initi-
ated by the enhanced perfusion and retention of cholesterol-rich, apoB-containing lipopro-
teins in the vessel wall [3]. These lipoproteins can be chemically modified by oxidation or
enzymatic cleavage increasing their pro-inflammatory and atherogenic potential. They are
cleared by extravasated monocyte-derived macrophages which, due to limited negative feed-
back, lead to expansion of the phagosome and transform into lipid laden foam cells that con-
tain a large quantity of lipid droplets [4, 5]. Macrophages are in addition able to export excess
cholesterol to extracellular acceptors such as high-density lipoprotein (HDL) particles in
reverse cholesterol transport. For this purpose they utilize the major HDL apolipoprotein
apoA-I and the ABC-transporters ABCA1 and ABCG1 as well as the scavenger receptor B1
(SR-BI) [6].

In the current study we used enzymatically modified low-density lipoproteins (eLDL) [7]
and oxidized low-density lipoproteins (oxLDL) [8, 9] to specifically mimic the properties of *in
vivo* occurring lipoprotein modifications. eLDL is characterized by proteolytic cleavage of
apoB and hydrolysis of core cholesteryl esters, leading to liposome-like, coreless LDL particles,
rich in unesterified cholesterol, free fatty acids and lysophospholipids. These particles resemble
lesion derived LDL present at early stages in atherosclerotic lesions and induce storage of cho-
lesteryl esters and triglycerides in lipid droplets leading to the "foamy" phenotype of macro-
phages [10]. In contrast, oxLDL particles are similar to polar surface modified particles found
in lesions [11]. Oxidation of LDL renders oxLDL resistant to lysosomal hydrolysis and traps
partially hydrolyzed oxLDL within the endolysosomal compartment [12], leading to phospho-
lipidosis [5, 13] and impaired release of cholesterol from lysosomes [14, 15]. The differential
composition and effects of eLDL and oxLDL have been reported recently [5, 10].

In the macrophage membrane, cholesterol loading leads to a deregulation of membrane
homeostasis inducing an altered membrane composition, which is a major event in atheroscle-
rotic progression [16]. Intracellular lipid flux and membrane lipid composition are essential
components of inflammatory signaling. Especially lipid rafts represent highly dynamic mem-
brane microdomains that play an essential role in transmembrane signaling. They modulate
the compartmentalization of signal transduction by facilitating or inhibiting the assembly of
signaling complexes [17]. Modest changes in their lipid composition are sufficient to induce
membrane and protein reorganization with subsequent signal transduction. The physiological
relevance of this process in immune cells could be shown for a variety of receptors and pro-
cesses. For example in macrophages the recruitment of TNF receptor 1 to lipid rafts is essential
for NF-kappa B activation [18]. Lipid rafts contain two to three-fold higher amounts of

cholesterol in comparison to the surrounding membrane and are also strongly enriched in sphingolipids and glycosphingolipids such as gangliosides [19]. Especially sphingomyelin that acts as a receptor for cholesterol is known to be essential for lipid raft formation and membrane functionality [20].

Sphingolipids are of special importance because they also influence the formation of atherosclerotic lesions by mediating lipoprotein uptake [21] and serving as precursors for signaling lipids [22]. They are ubiquitous and structurally diverse, based upon a common sphingobase backbone which can be N-acetylated to form ceramides (Cer). Further head group modifications lead to diverse glycosphingolipid and sphingomyelin (SM) species. Sphingomyelin is a major plasma membrane constituent that can strongly interact with unesterified cholesterol in animal cells. It can also serve as a cellular source for choline groups [23]. Ceramides can act as cellular mediators, regulating proliferative and apoptotic processes in the ceramide/sphingosine-1-phosphate rheostat via diverse signaling pathways including G-protein coupled receptor signaling [24, 25]. Ceramide biosynthesis is dependent either on *de novo* synthesis from palmitoyl CoA via sphinganine or sphingobase liberation from sphingosine-1-phosphate through the salvage pathway [26, 27]. Sphingomyelinase dependent conversion of sphingomyelin to ceramides is regarded as a starting signal for apoE mediated tissue remodeling of the damaged vasculature and in nerve injury [28–30].

In previous studies we examined lipid remodeling during phagocytic differentiation and compared *in vitro* lipoprotein loading of the two prototypic lipoproteins eLDL or oxLDL with unmodified LDL using lipidomics, transcriptomics, flow cytometry and fluorescent high-content imaging [31–35]. We could especially show that oxLDL increased ceramide and lactosylceramide expression leading to ceramide-rich membrane microdomains, whereas loading with eLDL induced sphingomyelin/cholesterol-rich membrane microdomains [13]. In the current study we therefore analyze these effects further in detail and look at underlying mechanisms as well as on membrane microdomains sphingolipid composition during differentiation, lipid loading and HDL_3 mediated deloading.

Materials and Methods

Chemical and enzymatic modification of low density lipoproteins

Isolation of human native LDL (1.006 mg/mL<d<1.063 mg/mL) from plasma of healthy blood donors and subsequent enzymatic degradation was performed as described previously [36] with slight modifications. Briefly, LDL was diluted to 2 mg/mL protein in PBS (w/o Ca^{2+}; Mg^{2+}). Enzyme treatment (eLDL) was conducted with trypsin (6.6 µg/mL) (Sigma, Germany) and cholesterol esterase (40 µg/mL) (Seikagaku, Japan) for 48 h at 37˚C. Oxidative modification (oxLDL) of LDL was performed according to published protocols [37] by dialyzing LDL (1 mg of protein per mL) against 5 µM $CuSO_4$. Modified lipoproteins were stored at 4˚C and used within a week. During LDL preparation and subsequent modification, general precautions were taken to avoid lipopolysaccharide (LPS) contamination.

Monocyte isolation, differentiation and lipid loading

Primary human monocytes were obtained from healthy normolipidemic volunteers with the apolipoprotein E3/E3 genotype by leukapheresis and counterflow elutriation as described previously [38]. The study was approved by the ethics committee of the University Hospital Regensburg and donors gave their written consent (Universitätsklinikum Regensburg, Ethikkommission der medizinischen Fakultät, proposal 08/119). Monocyte cultivation and differentiation was conducted according to Stoehr et al. [39]. Briefly, elutriated monocytes were seeded at 1x10^6 cells/mL in macrophage serum-free medium (Invitrogen, Germany)
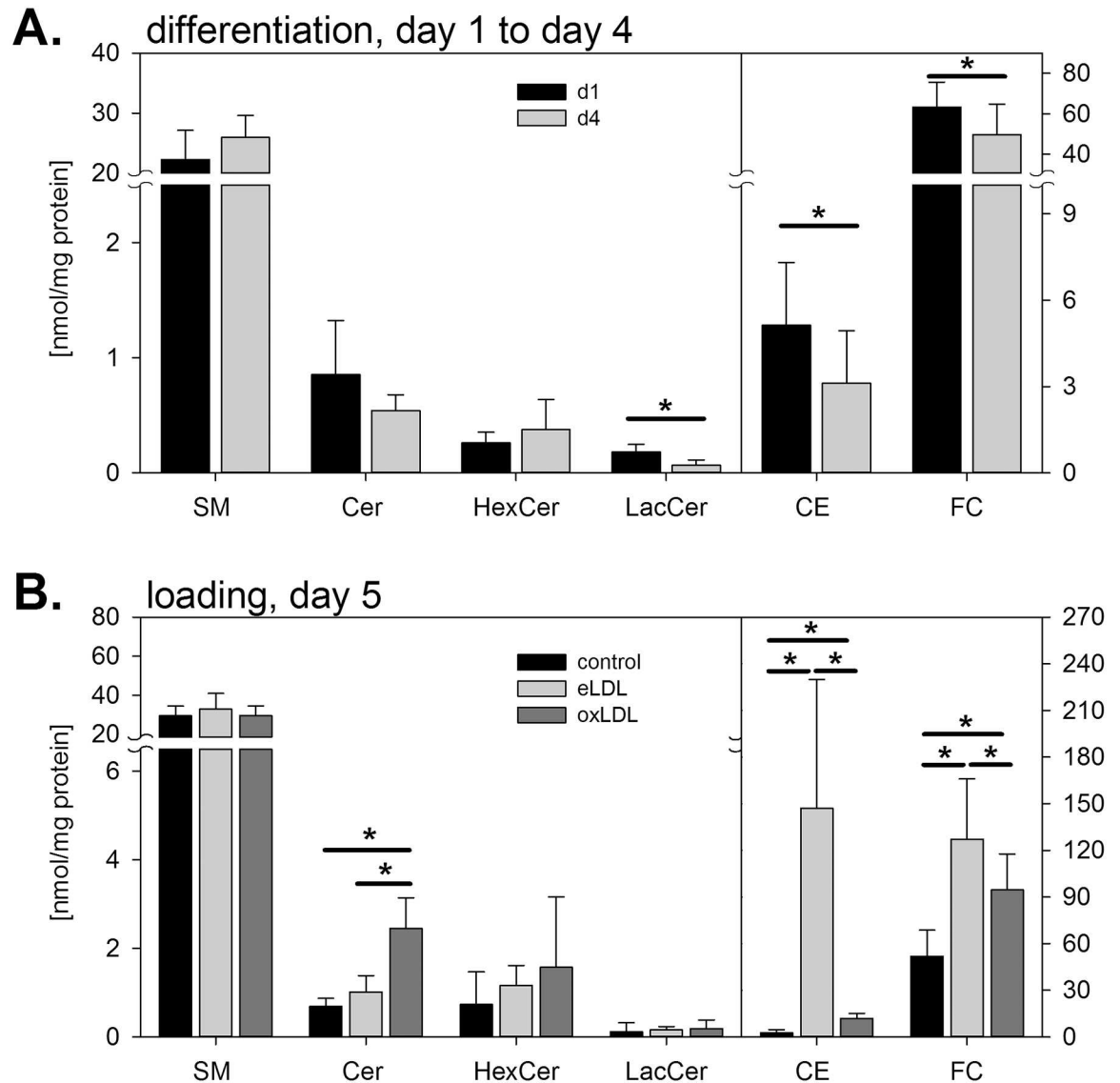
Fig 1. Quantitative mass spectrometric analysis of lipid classes. Lipid species composition of human blood monocytes was analyzed **(A)** on day one (d1) and four (d4) after MCSF differentiation and **(B)** following 24h enzymatically modified (eLDL) or oxidized (oxLDL) low density lipoprotein loading. Lipid classes include sphingomyelin (SM), ceramides (Cer), hexosylceramides (HexCer), lactosylceramides (LacCer), cholesteryl ester species (CE) and free cholesterol (FC). mean +/- SD. * = p< 0.05. n = 6.

doi:10.1371/journal.pone.0166798.g001

supplemented with 50 ng/mL recombinant human monocyte-colony stimulating factor (MCSF; R&D Systems, USA) to induce phagocytic differentiation. Cells were cultured either on plastic petri dishes (Sarstedt, USA), Ultra Low Attachment 6-well plates (Costar Corning, Germany), Cell+ 6-well plates (Sarstedt, USA) or Lab-Tek II glass chamber slides (Nalgen-eNunc Intl., USA) and incubated at 37°C/5% CO_2.

On the fourth day loading with eLDL (40 µg/mL) or oxLDL (80 µg/mL) was performed for either 24h in the lipidomic experiments (Fig 1 and S1 Fig) or for 48 h in all other experiments. Cells were harvested on day(s) one (initial state), four (MCSF differentiated) and six (loaded) respectively and analysis was performed. Cells were checked for apoptosis by flow cytometry using AnnexinV-FITC and propidium iodide (PI) staining.

For HDL$_3$ deloading, cells were first differentiated and incubated with LDL, eLDL or oxLDL as described previously. On day six, cells were washed and incubated with serum free medium containing MCSF and incubated another 24 h with HDL$_3$ (100 μg/mL) as described previously [40]. Cell harvest and analysis was performed as described previously for MCSF-differentiation and lipoprotein loading.

Lipid analysis

Lipid extraction at desired time points was performed by the method of Bligh and Dyer [41] or by butanolic extraction as described previously [42]. Mass spectrometry based targeted lipid analysis in the presence of isotopic labeled or not naturally occurring lipid species as internal standards was performed essentially as described previously [31, 42–46]. In brief, cells were washed twice in PBS, lysed in 0.1% SDS, sonicated and aliquots corresponding to each 100 μg total protein (BCA assay, Pierce, USA) were used for lipid extraction.

Direct flow injection utilized a 1100 series binary pump (Agilent, Germany) coupled via electrospray ionization (ESI) to a Quattro Ultima tandem mass spectrometer (Micromass, UK). HILIC LC-ESI-MS/MS was conducted using a 1200 series binary pump (Agilent, Germany) and a hybrid triple quadrupole linear ion trap mass spectrometer API 4000 Q-Trap (AB Sciex, Germany). Quantification was performed by standard addition calibration to cell homogenates using a number of naturally occurring lipid species for each lipid class. Lipid nomenclature was applied according to the notation proposed by Liebisch et al [47].

Quantitative PCR

Total RNA of harvested cells was isolated by RNeasy Mini Kits (Qiagen, Germany) and DNA digestion was performed on column. Integrity of the extracted RNA was verified on an Agilent 2100 bioanalyzer equipped with an RNA 6000 Nano LabChip reagent set (Agilent, Germany). Extracted RNA was quantified with a Nanodrop ND-1000 photometer (PeqLab, Germany). qPCR was performed using commercially available, predesigned TaqMan® PCR assays on the ABI Prism 7900 HT Sequence Detection System (Perkin Elmer-Applied Biosystems, Germany) according to manufacturer's instructions. For quantification we used the standard curve method. Therefore a stock of total RNA from macrophages was serially diluted and a standard curve with 50, 25, 12.5, 6.25 and 3.125 ng total RNA was generated for all to determine the relative expression of genes and 18s mRNA in each sample. Finally the results were normalized to the endogenous control 18sRNA. All experiments were performed in triplicates.

Western blotting

Antibodies against ABCA1 (clone: AB.H10, mouse), ABCG1 (synthetic peptides AA185-196 and AA347-362 against an internal region of human ABCG1/NP_058198, rabbit) or PLTP (mouse) were purchased from Abcam (UK), Pineda (Germany) or were a kind gift from M. Jauhiainen (National Public Health Institute, Department of Molecular Medicine, Helsinki, Finland), respectively. Cells were washed with PBS, frozen (-20°C), and thawed twice. Cell debris was separated by centrifugation at 10.000 x g for 10 min at 4°C. Proteins were separated by SDS-PAGE and transferred to PVDF (polyvinylindene fluoride) membranes. For detection of some proteins non reducing condition were necessary. Incubations with antibodies were performed in 5% nonfat dry milk in PBS, 0.1% Tween. Detection of the proteins was carried out with the ECL Western blot detection system and following quantification with the lumi-imager.

Staining of ceramide and acid sphingomyelinase

Cells cultured on coverslips were washed with PBS, fixed in 4% paraformaldehyde (15 min), quenched with 50 mM NH_4Cl/glycine (15 min) and blocked with PBS/0.5% BSA (15 min) at 20˚C. Afterwards, cells were incubated with anti-ceramide mAB (MID15B4, Alexis, Germany) for 4 h and labeled with anti-mouse Cy5 (Abcam, UK) for 1 h at 4˚C, followed by incubation with theta-toxin-FITC for 20 min at 4˚C (Competence center for fluorescence biology KFB, Regensburg, Germany) for cholesterol staining. SMPD1 staining was performed by incubation of fixed cells for 45 min with rabbit polyclonal anti-SMPD1 antibody (Santa Cruz Biotechnology, USA) at 2 µg/mL. Cells were then washed in PBS-BSA and stained for 45 min with 200 ng/mL 488 Alexa goat anti-rabbit antibody (Molecular Probes, Netherlands). Nonspecific fluorescence was excluded by performing controls without primary antibody. Control staining was performed without primary antibody. For sphingomyelin staining, cells were incubated with lysenin-His for 3 h at 4˚C followed by anti-His probe (H-15, Santa Cruz Biotechnology, USA) incubation for 2 h and subsequent incubation with anti-rabbit Texas Red for 30 min (Calbiochem, Germany).

Lysenin gene supplemented with His-tag at the N-terminus was synthesized and subcloned into pT7-7 plasmid and the recombinant protein was produced in *E. coli* [48]. All stainings were performed at 4˚C. Images were acquired with an inverted TCS-4D confocal microscope (Leica, Germany) equipped with an Ar/Kr 75 mV mixed-ion laser (MellesGriot/Omnichrome, USA) and observed with an oil immersion objective 100 x lens. Acquisition was performed with the Scan Ware software package of the instrument and analysis was done using the software Metamorph (Universal Imaging Corp., USA). Fluorescence images were acquired with a 488 nm laser line (excitation) detected with a 535/405 nm band pass filter (emission) and observed with an oil immersion objective Plan Apo 100x lens (NA 1.3).

Determination of cell surface ceramide

Cells were harvested gently from non-adherent dishes, washed with PBS (w/o Ca^{2+}; Mg^{2+}) and resuspended in PBS (w/o Ca^{2+}; Mg^{2+})/0.5% BSA to yield $5x10^6$ cells/mL. Flow-cytometric analysis of surface exposed ceramide of $5x10^5$ cells was performed. Cells were incubated for 15 minutes on ice with saturating concentrations of the antibodies against ceramide (MID15B4, Alexis), CDw17 (G035-FITC, Becton-Dickinson), CD65s (VIM2-FITC, Caltag) and CD77 (38–13, Immunotech). Monoclonal antibodies used for detection were directly fluorochrome-conjugated or indirectly labeled by subsequent incubation with fluorochrome-conjugated secondary reagents (ceramide: goat anti mouse-FITC, Becton-Dickinson; CD77: goat anti rat-PE, Dianova) after two washing steps with PBS containing 0.5% BSA. GM1 was stained using Alexa Fluor 488 labeled cholera toxin subunit B (Molecular Probes).

Detergent lysis and flotation gradient

Cells were harvested at the differentiated and eLDL and oxLDL loaded states, crude membrane fraction was isolated and Lubrol-WX detergent resistant microdomains were prepared as described previously [49]. These fractions were analyzed by ESI-MS/MS.

ApoE and apoA-I binding and uptake assay

After washing the cells with PBS, they were resuspended in PBS/0.5% BSA at $5 x 10^6$/ml and incubated with 10µg/ml of apoE-Cy3 and apoA-I-Cy5 at 4˚C and at 37˚C for 5 min. Then cells were washed three times with cold PBS/0.5% BSA and analyzed by flow cytometry.

Cells cultured on coverslips were washed with PBS and incubated with 10μg/ml of apoE-Cy3 and apoA-I-Cy5 at 4°C to 5 min and washed with cold PBS. Subsequently cells were fixed using 4% paraformaldehyde in PBS for 15 min on ice. Afterwards cells were washed with cold PBS and analyzed by confocal microscopy.

STED microscopy

Stimulated emission depletion (STED) microscopy was performed in cooperation with PD Dr. Harke and Prof. Dr. Hell at the Max Planck Institute for Biophysical Chemistry in Göttingen, Germany. A detailed description of the method can be found in [50].

Statistical analysis

Statistical analysis was performed in SPSS 21.0. Paired t-tests were used to identify significant changes between days 1 and day 4 of monocyte to macrophage differentiation. In these analyses no correction for multiple testing was considered necessary. In order to test for statistical significance between day 6 control, eLDL and oxLDL loaded cells repeated measure ANOVA with pairwise and a LSD corrected post-hoc comparison was conducted. For total HexCer species Greenhouse—Geisser correction was additionally applied because sphericity was violated according to Mauchly's test. Results are expressed as mean ± SD. Sigma Plot 12.5 and Excel 2010 were used for visualization.

Results

Transcriptomics shows increases in sphingolipid catabolic and decreases in sphingolipid biosynthetic transcripts during differentiation

While levels of total sphingomyelin (SM), ceramide (Cer) and hexosyl ceramide (HexCer) were not significantly altered during differentiation, total amounts of lactosyl ceramide (LacCer) and cholesteryl ester (CE) species as well as free cholesterol (FC) were significantly reduced (n = 6) (Fig 1A). Moreover, individual lipid species within sphingolipid classes were also significantly altered with increasing levels of SM 14:0, 24:3 and 24:2 species, while SM 15:0, 16:1, 18:0 and 22:0 decreased (S1A–S1D Fig). Concomitantly, Cer d18:1/18:0, 20:0, 22:0, 23:0 and 24:0 decreased, while HexCer d18:1/16:0 increased and LacCer 16:0, 22:0, 24:0 and 24:1 decreased during MCSF-dependent phagocytic differentiation.

During four days of MCSF-dependent monocyte/macrophage differentiation, mRNA expression of serine palmitoyltransferases 1+2 (SPTLC1+2), which are involved in ceramide de-novo synthesis as well as the transcriptional levels of sphingomyelin synthases, 1 and 2 which convert ceramides into sphingomyelin were downregulated (Fig 2A–2D). Analysis of the sphingomyelinases, which convert sphingomyelin to ceramide, revealed an upregulation of mRNA expression of acid sphingomyelinase (SMPD1) (2.8-fold) and acid sphingomyelinase like phosphodiesterase (ASML3B) (3.5-fold) (Fig 2E and 2F) whereas the mRNA expression of neutral sphingomyelinase (SMPD2) and neutral sphingomyelinase activation associated factor (NSMAF) was downregulated 1.5-fold during differentiation (Fig 2G and 2H). mRNA expression of glucosylceramidase (glucosidase beta acid, GBA) involved in the degradation of glucosylceramide into ceramide did not change during differentiation (Fig 2I). UDP-glucose ceramide glucosyltransferase (UGCG) the enzyme that converts ceramide to glucosylceramide and acid ceramidase (ASAH1) degrading ceramide to sphingosine showed an upregulation of mRNA expression (2 and 3.9-fold respectively) during differentiation (Fig 2J and 2K). The mRNA expression of sphingosine kinase 1 (SPHK1) which generates sphingosine-1-phosphate (S1P) from sphingosine was downregulated 1.5-fold (Fig 2M). In summary, upregulation of
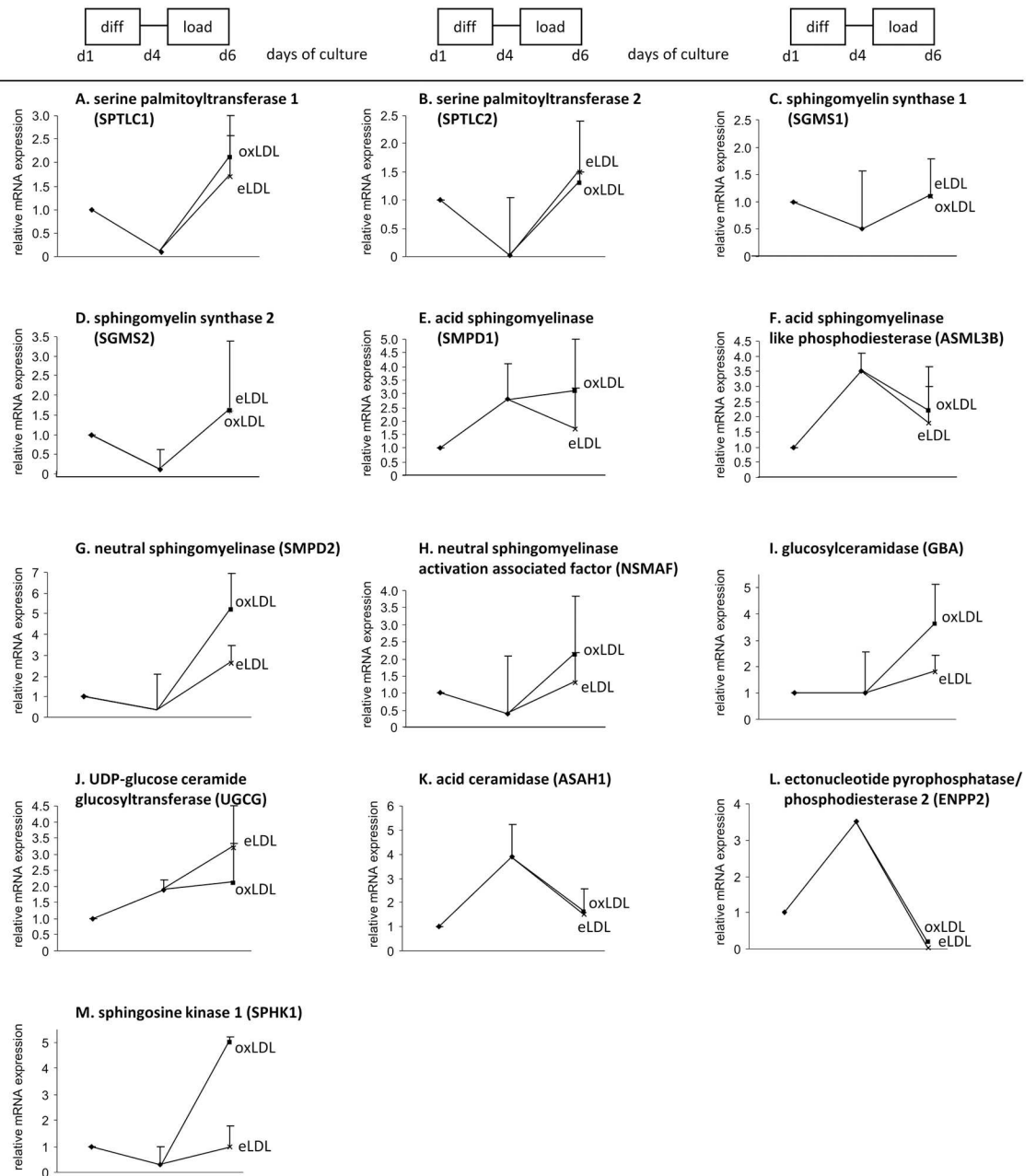
Fig 2. Taqman RT-PCR analysis of enzymes mainly involved in sphingolipid biosynthesis and metabolism. Gene expression was monitored of 4 day differentiated macrophages and of 48 hours eLDL and oxLDL loaded macrophages (day 4 to day 6. RT-PCR was standardized to 18s rRNA as a reference. mean + SD. n = 3.

sphingolipid catabolizing enzymes on the one hand (ASAH1, SMPD1, and ASML3B) and downregulation of sphingolipid synthesis pathway enzymes (SGMS1 and SGMS2) point towards reduced sphingolipid biosynthesis.

Taqman qPCR analysis and western blotting additionally showed a strong upregulation of the lipid transporters ABCA1 and ABCG1 during MCSF-dependent phagocytic differentiation (S2 Fig).

Loading with oxLDL increases cellular ceramides

While total sphingomyelin levels remained almost constant after loading with modified lipoproteins (Fig 1B), several individual sphingolipid species changed significantly with a similar pattern. Loading with eLDL significantly elevated sphingomyelin SM 15:0, 16:1, 18:0, 18:1, 20:1, 22:0, 22:2, 24:0 and 24:2 levels and oxLDL loading significantly increased mainly species containing saturated acyl-residues SM 14:0, 15:0, 16:1, 18:0, 18:1, 22:0, 24:0, 24:2 levels (S1E Fig).

Interestingly, only oxLDL led to a strong and significant increase of total ceramides as well as of multiple ceramide species (Cer d18:1/16:0, 18:0, 22:0, 23:0, 24:0, and 24:1, respectively), ranging between 3 to 5-fold, compared to control (S1F Fig). In contrast, eLDL significantly increased only Cer 18:1/22:0, 23:0 and 24:0. The most prominent elevations in ceramide species after lipoprotein loading were found in Cer d18:1/16:0 >24:1 > 24:0 > 22:0 > 23:0.

In addition, both eLDL (63-fold) and oxLDL (5-fold) significantly elevated most detectable cholesterylester species levels compared to control (Fig 1B and S1H Fig), resulting in an average total cholesterylester content of 147 nmol/mg for eLDL and 12 nmol/mg for oxLDL, respectively. Thus, eLDL loading was able to induce massive increases in cholesterylester species, while in oxLDL loaded cells the elevations were substantially lower but still significant.

Transcripts for the ceramide salvage pathway are upregulated by oxLDL

Ceramides are generated either by hydrolysis of sphingomyelin or reconversion of complex sphingolipids via sphingosine (salvage pathway) or *de novo* synthesized from palmitoyl-CoA via sphinganine and dihydroceramide using ceramide synthases and desaturases (S3 Fig). Acid and neutral sphingomyelinases are the enzymes that degrade sphingomyelin to ceramide within the salvage pathway. To elucidate the underlying reason for the ceramide elevation during oxLDL loading, TaqMan real-time RT-PCR was performed for the enzymes involved in ceramide generation and degradation in MCSF differentiated, as well as eLDL and oxLDL loaded macrophages.

During eLDL loading serine palmitoyltransferases 1 and 2 (SPTLC1, SPTLC2) were 1.7 and 1.5-fold and during oxLDL loading 2.1 and 1.3-fold upregulated (Fig 2A and 2B). Sphingomyelin synthase 1 was 1.1-fold and sphingomyelin synthase 2 was 1.6-fold upregulated during lipid loading independent of the lipoprotein (Fig 2C and 2D). SMPD1 and ASML3B mRNA expression was 1.7 and 1.8-fold downregulated during eLDL loading. oxLDL loading however revealed a 3.1-fold upregulation of SMPD1 and a 2.3-fold downregulation of ASML3B compared to MCSF. mRNA expression of SMPD2 and NSMAF showed a stronger upregulation during oxLDL loading (5.2- and 2.2-fold) than during eLDL loading (2.7- and 1.3-fold) (Fig 2G and 2H). The stronger upregulation of the sphingomyelinases SMPD1, SMPD2 and NSMAF during oxLDL loading compared with eLDL loading fits well with the oxLDL induced ceramide elevation. GBA was upregulated more strongly during oxLDL than during eLDL loading (3.7- vs 1.8-fold) (Fig 2I) also reflecting increased ceramide formation during oxLDL compared to eLDL loading. UGCG was higher upregulated during eLDL than during oxLDL loading (3.2- vs 2.2-fold) (Fig 2J) while SPHK1 was stronger upregulated during oxLDL than during eLDL loading (5- vs 1.2-fold) (Fig 2M) although no significant differences in sphingosine content were observable (S4 Fig).

No significant changes during eLDL and oxLDL loading could be found in the mRNA expression of serine palmitoyltransferase 1+2 (SPTLC1+2), sphingomyelin synthase, 1 and 2, N-acylsphingosine amidohydrolase 1 (ASAH1; acid ceramidase), sphingosine kinase 2 (SPHK2) and ectonucleotide pyrophosphate/phosphodiesterase 2 (ENPP2, autotaxin). The

mRNA expression of alkaline ceramidase and non-lysosomal ceramidase 2 (neutral ceramidase) was below the detection level.

Ceramides on the cell surface increase upon oxLDL loading

To investigate whether these adaptions also modulate ceramide and complex sphingolipid composition on the cell surface, flow cytometry was performed (Fig 3). During MCSF induced differentiation, surface quantities of ceramide, globotriaosylceramide/CD77 and GM1 ganglioside increased, while the amount of surface associated lactosylceramide/CDw17 and dodecasaccharideceramide/CD65s decreased.

Loading with oxLDL led to a strong increase in exposed surface ceramides and complex sphingolipids compared to MCSF differentiated macrophages while loading with eLDL only
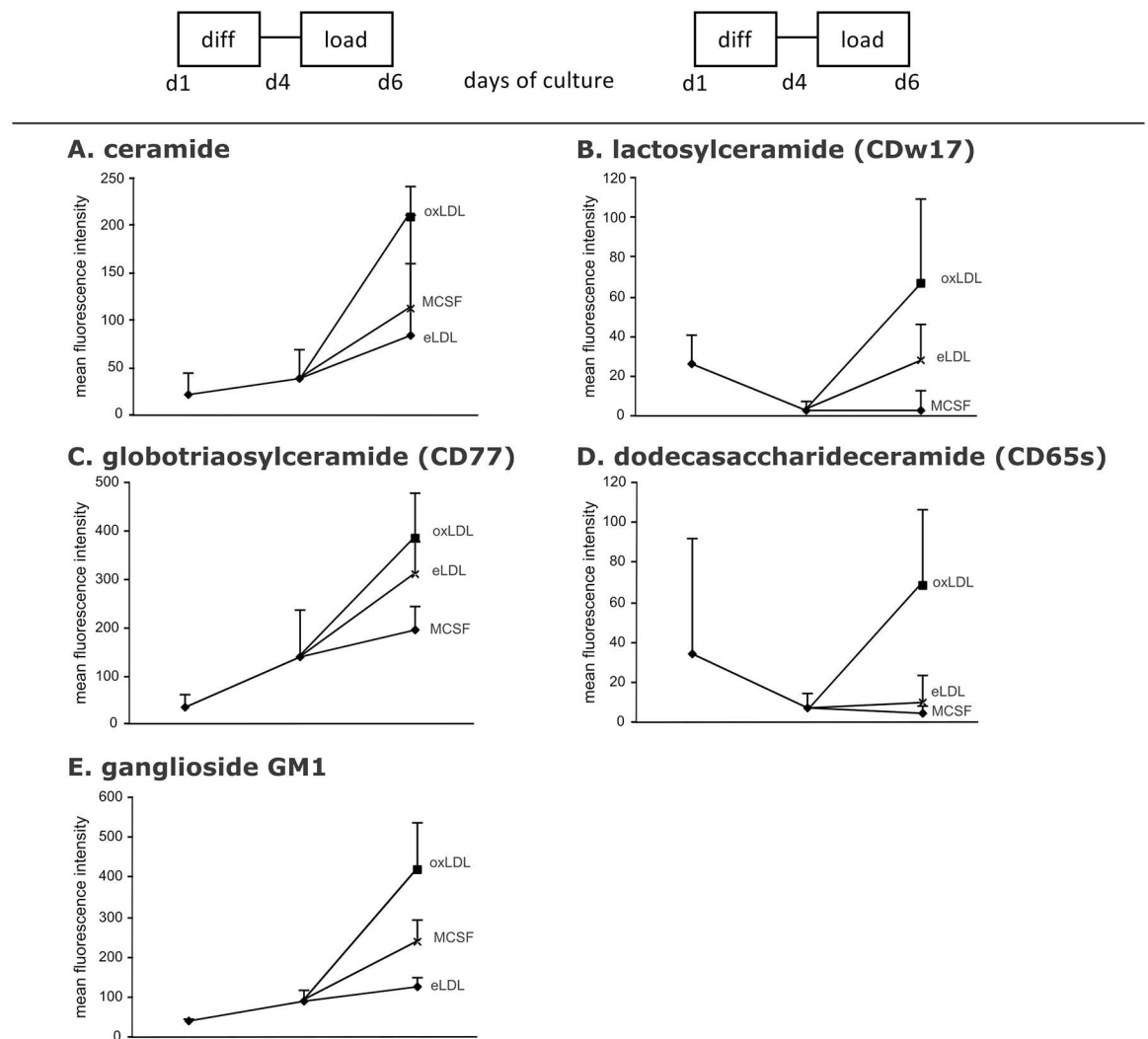

Fig 3. Cell surface expression of ceramide and complex sphingolipids. Depicted is the mean fluorescence intensity as analyzed by flow cytometry using monoclonal antibodies for ceramide, lactosylceramide globotriaosylceramide and dodecasaccharideceramide, and cholera toxin subunit B for ganglioside GM1 after MCSF differentiation (d4) and lipoprotein loading (d6) with eLDL, oxLDL or control (MCSF) **(A)** ceramide, **(B)** lactosylceramide/CDw17, **(C)** globotriaosylceramide, **(D)** dodecasaccharideceramide and **(E)** GM1 ganglioside. n = 3. Data on surface ceramide and lactosylceramide have been published previously [13].

doi:10.1371/journal.pone.0166798.g003

had a minor effect. These results indicate that oxLDL, in comparison to eLDL, not only increased total cellular ceramide content through the salvage pathway but also induced an increase in cell surface ceramides and complex sphingolipids. Ceramide-backbone glycosphingolipid surface expression was increased to a higher extent after oxLDL compared to eLDL loading.

oxLDL loading leads to higher SMPD1 levels on the cell surface

As mentioned above, qPCR analysis showed an upregulation in the transcription of acid sphingomyelin phosphodiesterase 1 (SMPD1) after loading of the cells with oxLDL as one potential reason for the increased membrane ceramide levels. SMPD1 is one of the key enzymes for the conversion of sphingomyelin to ceramide. We therefore hypothesized that not only increased expression but also increased cell surface SMPD1 could be responsible for this strong increase in membrane ceramides. To test this hypothesis SMPD1 protein localization was analyzed by confocal microscopy in MCSF treated, eLDL and oxLDL loaded macrophages (Fig 4). As anticipated oxLDL induced significantly higher cell surface ceramide fluorescence compared to control MCSF differentiation and loading with eLDL (Fig 4A). We additionally observed co-localization of ceramide with SMPD1 staining.

oxLDL induces microdomains enriched in cholesterol and ceramides

The surface distribution of cholesterol, sphingomyelin and ceramide was furthermore visualized by confocal microscopy (Fig 5). In addition to the anti-ceramide antibody clone MID15B4, theta toxin was used for the staining of cholesterol and lysenin for sphingomyelin labeling. Loading with eLDL and oxLDL induced a stronger staining of sphingomyelin compared to MCSF differentiated control cells. Compared to MCSF differentiated control cells, the amount and distribution of cholesterol was similar after eLDL and oxLDL loading. MID15B4 antibody staining showed that macrophages loaded with oxLDL presented the highest amount of ceramide in the membrane, indicating the formation of microdomains enriched in ceramide.

Visually the staining patterns of sphingomyelin and ceramide were consistent with membrane microdomains. The most widely used criterion to substantiate microdomain association is based on insolubility with detergents. We therefore investigated isolated Lubrol detergent resistant membranes (DRM) with ESI-tandem mass spectrometry. Under these conditions cholesterol based membrane domains are preserved. As shown in Fig 5F and 5G and Table 1, treatment with eLDL and oxLDL led to an induction of cholesterol rich DRMs compared to MCSF differentiation. Ceramide (Cer) and also hexosylceramide (HexCer) content of Lubrol DRMs was only significantly induced during oxLDL loading but not during eLDL loading. This is an indication for the specific formation of ceramide-rich membrane microdomains upon oxLDL loading. Elevations of sphingomyelin were generally less prominent and did not increase significantly for either treatment.

A co-localization of cholesterol and sphingomyelin could be observed mainly in cells loaded with eLDL and only to a lesser extent in oxLDL treated cells. This co-localization was abolished when the cells were deloaded with HDL_3 indicating a disruption of the raft structure. In contrast oxLDL loaded cells showed a large amount of cell surface domains rich in cholesterol and ceramides. Interestingly this co-localization of ceramide and cholesterol was not disrupted by HDL_3 mediated deloading.

Further evidence for the formation of membrane microdomains with a different lipid composition after loading with eLDL and oxLDL was obtained by stimulated emission depletion (STED) nanomicroscopy in collaboration with Prof Hell/PD Dr Harke at the MPI in
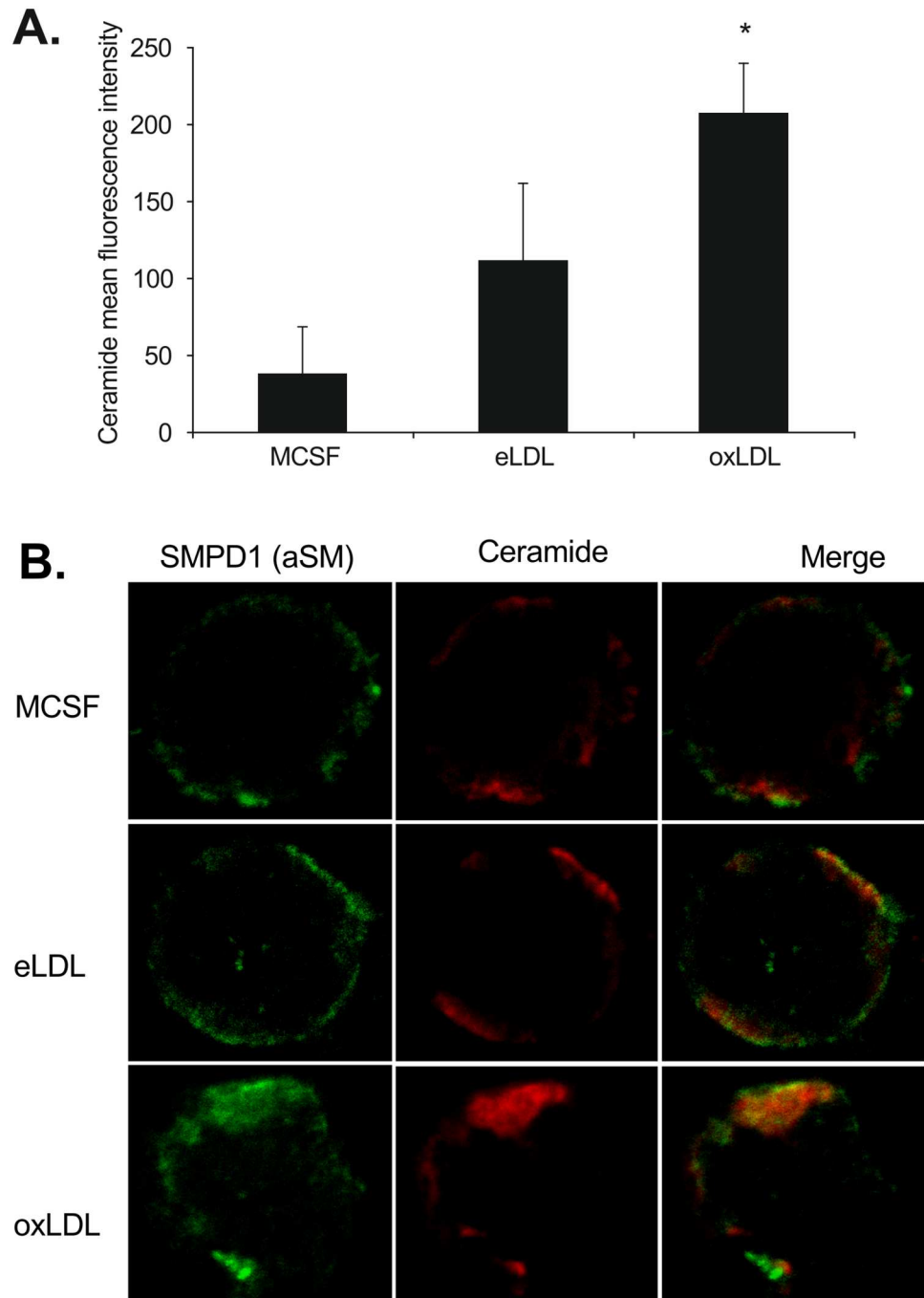
Fig 4. oxLDL induces cell surface ceramides and SMPD1 co-localization at the membrane. (A) Mean fluorescence intensity of MID15B4 labeled ceramide in MCSF treated, eLDL or oxLDL loaded macrophages. p < 0.05. **(B)** SMPD1 (aSM) surface expression (green) and cell surface ceramide content and distribution (red) after MCSF differentiation, eLDL or oxLDL loading. Merge: orange. Representative cells are shown.

Göttingen. For this purpose an antibody against FcγRIIA (CD32) was used to selectively stain membrane microdomains. This method revealed a cluster size of ceramide enriched microdomains between 30 and 50nm with a tendency of enlargement upon lipid loading compared to MCSF differentiation (S5 Fig).
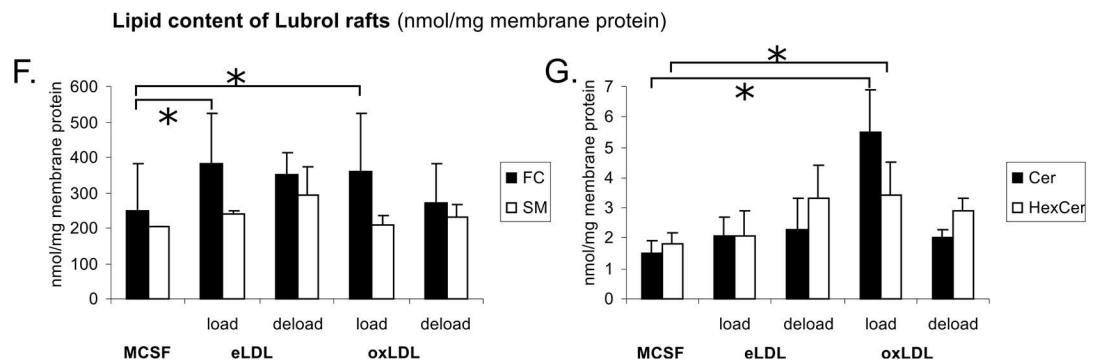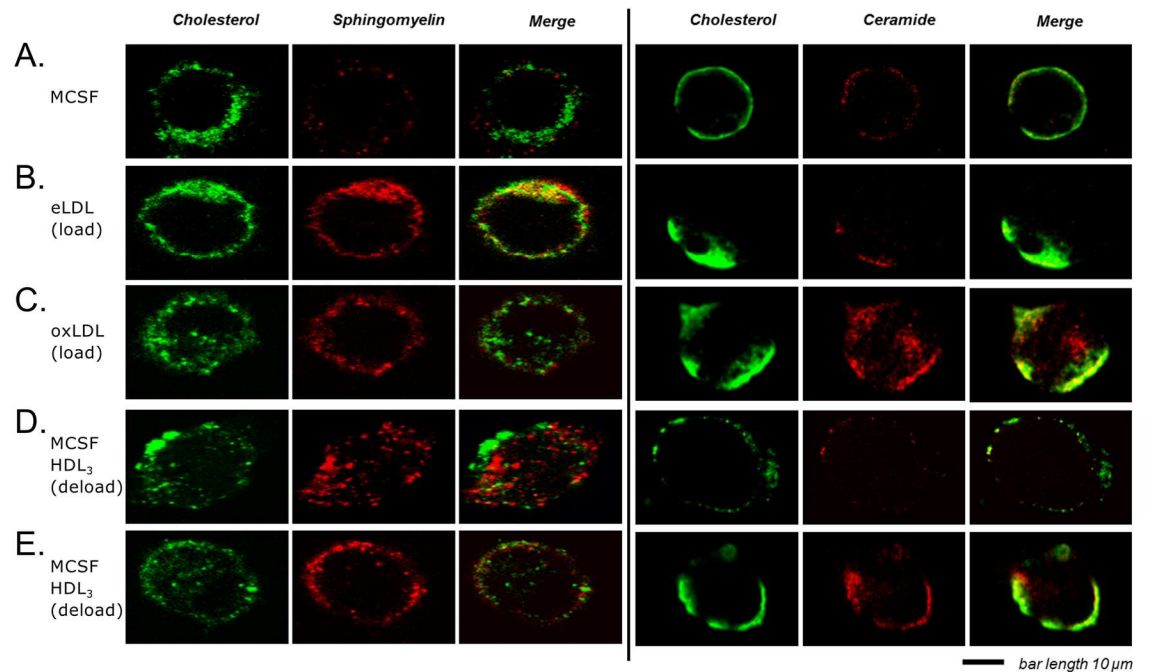
Fig 5. eLDL promotes formation of cholesterol/sphingomyelin rich membrane microdomains while oxLDL induces cholesterol/ceramide microdomains. (A) MCSF differentiation, **(B)** eLDL loading, **(C)** oxLDL loading, **(D)** eLDL loading with subsequent HDL$_3$-deloading and **(E)** oxLDL loading with subsequent HDL$_3$-deloading. Theta toxin was used for cholesterol and lysenin for sphingomyelin labeling. MID15B4 antibody was used for ceramide. Representative cells are shown.

doi:10.1371/journal.pone.0166798.g005

Table 1. Quantitative determination of the lipid content of Lubrol rafts.

	FC	SM	Cer	HexCer
MCSF (diff)	247 +/- 136	206 +/- 10	1.5 +/- 0.4	1.8 +/- 0.4
eLDL (load)	383 +/- 142 *	238 +/- 11	2.1 +/- 0.6	2.1 +/- 0.8
eLDL (deload)	349 +/- 66	295 +/- 77	2.3 +/- 1.0	3.3 +/- 1.1
oxLDL (load)	358 +/- 168 *	208 +/- 28	5.5 +/- 1.4 *	3.4 +/- 1.1 *
oxLDL (deload)	272 +/- 111	231 +/- 37	2.0 +/- 0.3	2.9 +/- 0.4

Free cholesterol (FC), sphingomyelin (SM), ceramide (Cer), hexosylceramice (HexCer). Values are given in nmol/mg protein.

* $p < 0.05$ compared to MCSF using Student's t-test. n = 3

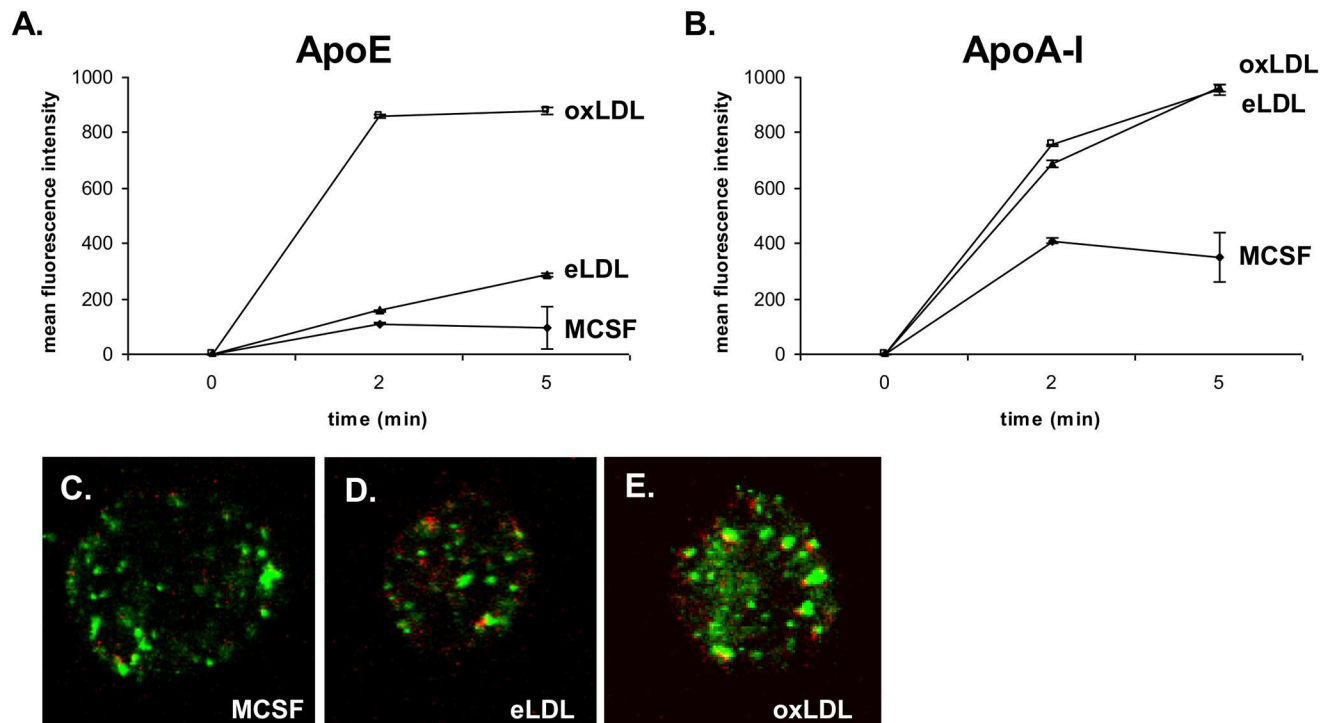doi:10.1371/journal.pone.0166798.t001

Fig 6. Binding and uptake of apoE and apoA-I determined by flow cytometry and confocal microsopy. 4°C binding of fluorescent labeled apoE (Cy3-apoE) **(A)** and apoA-I (Cy5-apoA-I) **(B)**. Flow cytometry was performed on control macrophages as well as on lipid loaded cells after 2 and 5 min in three independent different experiments. Additionally using confocal microsopy, binding of fluorescent labeled apoE (Cy3-apoE, green staining) and apoA-I (Cy5-apoA-I, red staining) was visualized following M-CSF differentiation **(C)** as well as after eLDL **(D)** and oxLDL **(E)** loading.

doi:10.1371/journal.pone.0166798.g006

ApoE binding to oxLDL treated cells is facilitated

As described previously by Morita et al [29], apoE preferentially binds to ceramide enriched domains compared to sphingomyelin-enriched domains on emulsion particle surfaces. We therefore analyzed 4°C binding uptake of fluorescent labelled apoE (Cy3-apoE) and apoA-I (Cy5-apoA-I) in MCSF differentiated, eLDL and oxLDL loaded macrophages by flow cytometry and confocal microscopy. Flow cytometry revealed a strongly enhanced binding of apoE to oxLDL loaded cells (Fig 6A) consistent with increased levels of surface ceramides. In contrast to apoE, apoA-I exhibited a comparable binding capacity at 4°C to eLDL and oxLDL loaded cells (Fig 6B). Confocal microsopy likewise showed a stronger fluorescence of Cy3-labeled apoE (green fluorescence) with oxLDL loaded cells compared to control and eLDL treated cells (Fig 6C–6E). Using Cy5-apoA-I a generally weaker staining was observed.

Discussion

Phagocytic differentiation had only minor effects on the cellular sphingolipid composition. Levels of total sphingomyelin and total ceramides remained unchanged, while free cholesterol as the major determinant of membrane fluidity decreased. This altered membrane fluidity most likely prepares the cell for its phagocytic function [51].

In contrast, treatment with free cholesterol-rich eLDL particles promoted foam cell formation while loading with oxLDL predominantly provoked endo-lysosomal cholesterol accumulation with characteristics of phospholipidosis most likely due to inhibition of lysosomal hydrolases and release of cholesterol from these organelles [52]. As a result oxLDL leads to a

dysfunction of vesicular trafficking with endolysosomal phospholipidosis and impaired cholesterol efflux [10, 12, 14, 32]. All further measurements were interpreted based on the assumption that lipids from eLDL and oxLDL particles are taken up about equally. A higher concentration of oxLDL was used because the cholesterol loading efficiency of eLDL is excessively higher as compared to oxLDL [53]. Therefore, to achieve a significant oxLDL dependent cholesterol effect we used a lower concentration of eLDL and the same concentration of oxLDL as in other publications (e.g. [54, 55]).

eLDL induced 54-fold higher levels of esterified cholesterol compared to unloaded control cells, while oxLDL showed only a 4.4-fold increase of CE species. Interestingly oxLDL increased the CE species 18:1 more than expected from the total increase. Free cholesterol was also elevated stronger by treatment with eLDL than by oxLDL but to a generally lower extent (2.5-fold and 1.8-fold respectively). These changes are in accordance with previously published data showing that eLDL due to the treatment with cholesterylester-hydrolase (acid lipase) contained a higher amount of FC at the expense of CE compared to LDL and oxLDL [56].

In contrast oxLDL loading of macrophages led to an upregulation of cellular ceramide content. On the species level, ceramides 16:0, 18:0, 20:0, 22:0, 23:0, 24:1 and 24:0 increased significantly around 3.7-fold. Likewise the specific cell surface ceramide composition at the plasma membrane was affected as shown by flow cytometry and fluorescence microscopy. On the other hand total cellular sphingomyelin content remained constant after lipoprotein loading, while plasma membrane sphingomyelin was increased after both eLDL and oxLDL lipoprotein loading.

eLDL and oxLDL particles have a comparable ceramide and sphingomyelin composition, therefore the increase in ceramides cannot be attributed to differential uptake of sphingolipids from the lipoprotein [56]. An endogenous source of ceramides in a mammalian cell is the sphingomyelin-ceramide rheostat. Ceramide can be released from complex sphingolipids leading to increases in ceramide and decreases in sphingolipid levels. Previously it has been shown that oxLDL can induce this mechanism by stimulation of neutral and acid SMase [57]. Oxysterols as exclusive components of oxLDL could additionally contribute to the elevation of cellular ceramide levels [58]. Our experiments are consistent with these observations and demonstrate that the mRNA expression of acid SMase, neutral SMase and neutral SMase activation associated factor is stronger upregulated during oxLDL compared to eLDL loading. Therefore the transcriptomic basis for an activation of the salvage pathway and not *de novo* synthesis as the reason for the increased ceramide levels after loading with oxLDL could be shown experimentally within the scope of this study. Naturally in the complex cellular environment, subsequent protein levels and further regulation of enzyme activity by additional factors such as gluthathion need to be considered.

oxLDL is taken up via scavenger receptors CD36, SR-A, SR-B, LOX-1 into early endosomes and in contrast to eLDL not stored in lipid droplets but exerts direct effects on transcription [10]. Exogenous sphingolipid can then be processed to ceramide and induce caspases and PLA$_2$. oxLDL effects are also, at least in part, mediated through the transcription factors PPAR-γ and NF-κB. Various bioactive oxidized lipids in oxLDL, such as 9-HODE and 13-HODE, are known to trigger NF-κB activation [59]. Likewise, oxLDL has a much higher content of Lysophosphatidylcholine (Lyso-PC) in comparison to unmodified LDL [56]. Lyso-PC can stimulate protein kinase C and tyrosine kinases leading to subsequent NF-κB activation [60]. Also bioactive oxysterols (especially 7-keto, 7-hydroxy and 25-hydroxycholesterol) are present in oxLDL [61]

Using confocal microscopy we found an accumulation of SMPD1 at the cell surface. SMPD1 is usually found in the endolysosomal compartment, but translocation to sphingolipid rich membrane microdomains converting them into ceramide rich microdomains that

facilitate receptor clustering is well established [62–64]. Sudden increases in ceramide levels due to the action of plasma membrane associated SMase may have an important impact on macrophage cholesterol homeostasis, bacterial host defense, and apoptosis [65].

Besides increased ceramide production after oxLDL loading we provide data that oxLDL induced microdomains are enriched in cholesterol and ceramides while microdomains in cells treated with eLDL have higher levels of cholesterol. Sphingomyelin was not increased significantly in Lubrol rafts from eLDL loaded cells, only a tendency was visible. Ceramide associates strongly with lipid rafts and stabilizes them. This can induce the formation of unusually large membrane domains in plasma membranes detectable by the monoclonal ceramide antibody which we used for our experiments [62]. In studies using lipid vesicles it was found that natural and saturated synthetic ceramides displace cholesterol from lipid microdomains [66]. In our macrophage experiments we detected a co-localization of cholesterol and ceramide mainly during oxLDL loading indicative for the coexistence of cholesterol and ceramide in membrane microdomains. In collaboration with Prof Hell/PD Harke, MPI Göttingen, we have furthermore performed pilot experiments with STED-nanomicroscopy which allows a spatial resolution of 30–70 nm. In our experiments we used a staining with an anti-FcγRIIa (CD32) antibody to visualize lipid rafts. CD32 is a polymorphic transmembrane glycoprotein that is characteristically associated with cholesterol-rich membrane subdomains [67]. Using this method we found a ceramide membrane microdomain size between 30 and 50 nm with a tendency to enlarge upon lipid loading.

oxLDL also exerts oxidative stress on the macrophage membrane. Previous experiments using H_2O_2 as a stimulus could demonstrate an increase in the number, but not the size, of membrane microdomains, therefore an involvement of survival pathways was assumed [68]. Moreover the major oxysterol in oxLDL, 7-ketocholesterol is able to activate src kinase [69] by cholesterol depletion and raft disruption [70].

In addition to the higher buildup of cell surface ceramide during oxLDL loading compared to eLDL loading, an increase of ceramide derived glycosphingolipids and GM1 ganglioside as detected by cholera toxin was measurable. This could reflect either increased net synthesis from ceramide or enhanced translocation from the Golgi to the plasma membrane during oxLDL loading. Alternatively, impaired degradation of glycosphingolipids or decreased endocytosis could also play a role. A little care needs to be taken in interpreting the staining of GM1 using cholera toxin. Although this method is widely used and GM1 represents the most efficient ligand, binding of cholera toxin to other glycosphingolipids, such as GD1b, fucosyl-GM1, B-GM1, GM2, GT1b, GD1a, GM3 and asiolo-GM1 have been reported in the literature and cannot be ruled out [71–75].

As a physiological consequence of the altered surface expression of ceramide and the differential membrane lipid microdomain formation during eLDL and oxLDL loading we demonstrated a stronger affinity of apoE to cells treated with oxLDL as compared to eLDL treated cells. Since ApoE staining was not only observable at the cell membrane also internalization of the lipoprotein seems reasonable to assume. Furthermore a more pronounced fluorescence in oxLDL treated cells is consistent with the observation that apoE preferentially binds to ceramide enriched membrane domains of emulsion particles treated with sphingomyelinase and not to sphingomyelin emulsion particles [29]. It is also compatible with the interaction of apoE and ceramides during nerve regeneration and remyelination [30]. ApoA-I binding however, was identical between eLDL and oxLDL loaded macrophages. This indicates that binding of extracellular apoA-I does not depend on microdomain ceramide content and may rather correlate with membrane cholesterol [76].

Endogenously synthesized ceramide and sphingomyelin enhances cellular cholesterol efflux to apoA-I by increasing the presence of ABCA1 at the cell surface [77]. This leads to a block of

the transport of CD36 to the plasma membrane preventing further uptake of oxLDL [78]. In our experiments we detected a strong induction of ABCA1 mRNA and protein in lipoprotein loaded cells. Especially loading with oxLDL induced a considerable increase in cellular ABCA1, consistent with endolysosomal storage of oxLDL and an expansion of the trans-Golgi network. Treatment with apoAI also has the potential to increase caveolar cholesterol by inducing a stronger mobilization from intracellular sources than promoting its efflux [79]. ABCA1 in macrophages, by reducing membrane cholesterol has been described to reduce toll-like receptor trafficking to lipid rafts and in this way moderate inflammation [80]. In contrast ABCA1 deficient macrophages have enlarged, cholesterol rich lipid microdomains with higher levels of TLR4 and an increased reactivity to lipopolysaccharides [81].

ApoE respectively apoE-rich lipoproteins such as VLDL, chylomicron remnants and HDL_1 also contribute to presentation of lipid antigens by high affinity binding of endogenous or exogenous antigens mainly ceramide derived glycosphingolipids [82]. Therefore higher apoE binding to ceramide rich membrane microdomains of oxLDL loaded macrophages may also promote antigen presentation and immune modulation.

Conclusions

In summary, we could demonstrate that the two atherogenic lipoprotein modifications eLDL and oxLDL induce two different types of lipid membrane microdomains in human macrophages. These changes are caused most likely by an induction of sphingomyelinases due to an activation of the salvage pathway as well as an increased translocation of acid sphingomyelinase to the plasma membrane. The formation of cholesterol/ceramide rich microdomains during oxLDL loading leads to a higher cell surface binding of apoE in contrast to the uniform affinity of apoA-I which could contribute to impaired lipid efflux and enhancement of inflammatory processes. This supports the view that differential formation of lipid membrane microdomains in macrophages could lead to differential functional responses towards atherogenesis.

Supporting Information

S1 Fig. Quantitative mass spectrometric analysis of individual lipid species during differentiation and loading. Lipid species content of extravasated blood monocytes was analyzed after four days phagocytic differentiation (A-D) or after 24 h lipoprotein loading (E-H) with eLDL or oxLDL, respectively. SM annotation is based on the assumption that sphingosine d18:1 is present. Mean +/- SD. * = $p < 0.05$. n = 6.
(PDF)

S2 Fig. Relative gene expression and protein levels of (A) ABCA1, (B) ABCG1 and (C) PLTP. Gene expression was analyzed using TaqMan RT-PCR analysis. Results are presented as mean +/- SD. Protein levels were assessed using Western Blot analysis with appropriate antibodies. Reference protein expression of ATP-Synthase is depicted in (D). n = 3.
(PDF)

S3 Fig. Ceramide synthesis and degradation pathways.
(PDF)

S4 Fig. Levels of sphingosine during monocyte to macrophage differentiation and after loading with lipoproteins.
(PDF)

S5 Fig. Determination of CD32 labeled membrane microdomain sizes by STED microscopy.
(PDF)

Author Contributions

Conceptualization: SW MG EO GS.

Formal analysis: SW MG MP.

Funding acquisition: GS.

Investigation: SW MG MP GL A. Sigrüner.

Methodology: SW MG GL EO A. Sigrüner A. Sobota GS.

Resources: A. Sobota.

Visualization: SW MG MP.

Writing – original draft: SW MG MP GS.

Writing – review & editing: SW GL GS.

References

1. Lloyd-Jones D, Adams RJ, Brown TM, Carnethon M, Dai S, De Simone G, et al. Executive summary: heart disease and stroke statistics—2010 update: a report from the American Heart Association. Circulation. 2010; 121(7):948. doi: 10.1161/CIRCULATIONAHA.109.192666 PMID: 20177011

2. Virmani R, Burke AP, Kolodgie FD, Farb A. Vulnerable plaque: the pathology of unstable coronary lesions. Journal of interventional cardiology. 2002; 15(6):439–46. PMID: 12476646

3. Moore KJ, Tabas I. Macrophages in the pathogenesis of atherosclerosis. Cell. 2011; 145(3):341–55. doi: 10.1016/j.cell.2011.04.005 PMID: 21529710

4. Williams KJ, Tabas I. The response-to-retention hypothesis of early atherogenesis. Arteriosclerosis, thrombosis, and vascular biology. 1995; 15(5):551–61. PMID: 7749869

5. Orsó E, Grandl M, Schmitz G. Oxidized LDL-induced endolysosomal phospholipidosis and enzymatically modified LDL-induced foam cell formation determine specific lipid species modulation in human macrophages. Chemistry and physics of lipids. 2011; 164(6):479–87. doi: 10.1016/j.chemphyslip.2011.06.001 PMID: 21683693

6. Schmitz G, Grandl M. The molecular mechanisms of HDL and associated vesicular trafficking mechanisms to mediate cellular lipid homeostasis. Arteriosclerosis, thrombosis, and vascular biology. 2009; 29(11):1718–22. doi: 10.1161/ATVBAHA.108.179507 PMID: 19846837

7. Bhakdi S, Dorweiler B, Kirchmann R, Torzewski J, Weise E, Tranum-Jensen J, et al. On the pathogenesis of atherosclerosis: enzymatic transformation of human low density lipoprotein to an atherogenic moiety. The Journal of experimental medicine. 1995; 182(6):1959–71. PMID: 7500042

8. Witztum JL. The oxidation hypothesis of atherosclerosis. The Lancet. 1994; 344(8925):793–5.

9. Witztum JL, Steinberg D. Role of oxidized low density lipoprotein in atherogenesis. Journal of Clinical Investigation. 1991; 88(6):1785. doi: 10.1172/JCI115499 PMID: 1752940

10. Schmitz G, Grandl M. Endolysosomal phospholipidosis and cytosolic lipid droplet storage and release in macrophages. Biochimica et Biophysica Acta (BBA)-Molecular and Cell Biology of Lipids. 2009; 1791 (6):524–39.

11. Boullier A, Li Y, Quehenberger O, Palinski W, Tabas I, Witztum JL, et al. Minimally oxidized LDL offsets the apoptotic effects of extensively oxidized LDL and free cholesterol in macrophages. Arteriosclerosis, thrombosis, and vascular biology. 2006; 26(5):1169–76. doi: 10.1161/01.ATV.0000210279.97308.9a PMID: 16484596

12. Jessup W, Wilson P, Gaus K, Kritharides L. Oxidized lipoproteins and macrophages. Vascular pharmacology. 2002; 38(4):239–48. PMID: 12449020

13. Grandl M, Bared SM, Liebisch G, Werner T, Barlage S, Schmitz G. E-LDL and Ox-LDL differentially reg-
     ulate ceramide and cholesterol raft microdomains in human Macrophages. Cytometry Part A. 2006; 69
     (3):189–91.

14. Gelissen IC, Brown AJ, Mander EL, Kritharides L, Dean RT, Jessup W. Sterol efflux is impaired from
     macrophage foam cells selectively enriched with 7-ketocholesterol. Journal of Biological Chemistry.
     1996; 271(30):17852–60. PMID: 8663356

15. Maor I, Mandel H, Aviram M. Macrophage Uptake of Oxidized LDL Inhibits Lysosomal Sphingomyeli-
     nase, Thus Causing the Accumulation of Unesterified Cholesterol—Sphingomyelin—Rich Particles in
     the Lysosomes A Possible Role for 7-Ketocholesterol. Arteriosclerosis, thrombosis, and vascular biol-
     ogy. 1995; 15(9):1378–87. PMID: 7670952

16. Shibata N, Glass CK. Macrophages, oxysterols and atherosclerosis. Circulation journal: official journal
     of the Japanese Circulation Society. 2010; 74(10):2045–51.

17. Simons K, Toomre D. Lipid rafts and signal transduction. Nature reviews Molecular cell biology. 2000; 1
     (1):31–9. doi: 10.1038/35036052 PMID: 11413487

18. Legler DF, Micheau O, Doucey M-A, Tschopp J, Bron C. Recruitment of TNF receptor 1 to lipid rafts is
     essential for TNFα-mediated NF-κB activation. Immunity. 2003; 18(5):655–64. PMID: 12753742

19. Pike LJ. Lipid rafts bringing order to chaos. Journal of lipid research. 2003; 44(4):655–67. doi: 10.1194/
     jlr.R200021-JLR200 PMID: 12562849

20. Kulma M, Herec M, Grudzinski W, Anderluh G, Gruszecki WI, Kwiatkowska K, et al. Sphingomyelin-rich
     domains are sites of lysenin oligomerization: implications for raft studies. Biochim Biophys Acta. 2010;
     1798(3):471–81. Epub 2009/12/19. doi: 10.1016/j.bbamem.2009.12.004 PMID: 20018171.

21. Park T-S, Panek RL, Rekhter MD, Mueller SB, Rosebury WS, Robertson A, et al. Modulation of lipopro-
     tein metabolism by inhibition of sphingomyelin synthesis in ApoE knockout mice. Atherosclerosis. 2006;
     189(2):264–72. doi: 10.1016/j.atherosclerosis.2005.12.029 PMID: 16458317

22. Clarke C, Cloessner E, Roddy P, Hannun Y. Neutral sphingomyelinase 2 (nSMase2) is the primary neu-
     tral sphingomyelinase isoform activated by tumour necrosis factor-alpha in MCF-7 cells. Biochem J.
     2011; 435:381–90. doi: 10.1042/BJ20101752 PMID: 21303347

23. Merrill AH Jr, Jones DD. An update of the enzymology and regulation of sphingomyelin metabolism.
     Biochimica et Biophysica Acta (BBA)-Lipids and Lipid Metabolism. 1990; 1044(1):1–12.

24. Rivera J, Proia RL, Olivera A. The alliance of sphingosine-1-phosphate and its receptors in immunity.
     Nat Rev Immunol. 2008; 8(10):753–63. Epub 2008/09/13. doi: 10.1038/nri2400 PMID: 18787560;
     PubMed Central PMCID: PMC2600775.

25. Fenger M, Linneberg A, Jorgensen T, Madsbad S, Sobye K, Eugen-Olsen J, et al. Genetics of the cer-
     amide/sphingosine-1-phosphate rheostat in blood pressure regulation and hypertension. BMC Genet.
     2011; 12:44. Epub 2011/05/17. doi: 10.1186/1471-2156-12-44 PMID: 21569466; PubMed Central
     PMCID: PMC3115901.

26. Paumen MB, Ishida Y, Muramatsu M, Yamamoto M, Honjo T. Inhibition of carnitine palmitoyltransferase
     I augments sphingolipid synthesis and palmitate-induced apoptosis. Journal of Biological Chemistry.
     1997; 272(6):3324–9. PMID: 9013572

27. Pettus BJ, Chalfant CE, Hannun YA. Ceramide in apoptosis: an overview and current perspectives. Bio-
     chimica et Biophysica Acta (BBA)-Molecular and Cell Biology of Lipids. 2002; 1585(2):114–25.

28. Morita S-y, Kawabe M, Sakurai A, Okuhira K, Vertut-Doï A, Nakano M, et al. Ceramide in lipid particles
     enhances heparan sulfate proteoglycan and low density lipoprotein receptor-related protein-mediated
     uptake by macrophages. Journal of Biological Chemistry. 2004; 279(23):24355–61. doi: 10.1074/jbc.
     M402035200 PMID: 15044445

29. Morita S-y, Nakano M, Sakurai A, Deharu Y, Vertut-Doï A, Handa T. Formation of ceramide-enriched
     domains in lipid particles enhances the binding of apolipoprotein E. FEBS letters. 2005; 579(7):1759–
     64. doi: 10.1016/j.febslet.2005.02.018 PMID: 15757672

30. Boyles JK, Zoellner CD, Anderson LJ, Kosik LM, Pitas RE, Weisgraber K, et al. A role for apolipoprotein
     E, apolipoprotein AI, and low density lipoprotein receptors in cholesterol transport during regeneration
     and remyelination of the rat sciatic nerve. Journal of Clinical Investigation. 1989; 83(3):1015. doi: 10.
     1172/JCI113943 PMID: 2493483

31. Ecker J, Liebisch G, Englmaier M, Grandl M, Robenek H, Schmitz G. Induction of fatty acid synthesis is
     a key requirement for phagocytic differentiation of human monocytes. Proceedings of the National
     Academy of Sciences. 2010; 107(17):7817–22.

32. Grandl M, Schmitz G. Fluorescent high-content imaging allows the discrimination and quantitation of E-
     LDL-induced lipid droplets and Ox-LDL-generated phospholipidosis in human macrophages. Cytometry
     Part A. 2010; 77(3):231–42.

33. Wolf Z, Orsó E, Werner T, Klünemann H, Schmitz G. Monocyte cholesterol homeostasis correlates with the presence of detergent resistant membrane microdomains. Cytometry Part A. 2007; 71(7):486–94.

34. Schmitz G, Grandl M. Role of redox regulation and lipid rafts in macrophages during Ox-LDL-mediated foam cell formation. Antioxidants & redox signaling. 2007; 9(9):1499–518.

35. Wallner S, Grandl M, Konovalova T, Sigrüner A, Kopf T, Peer M, et al. Monocyte to Macrophage Differentiation Goes along with Modulation of the Plasmalogen Pattern through Transcriptional Regulation. PloS one. 2014; 9(4):e94102. doi: 10.1371/journal.pone.0094102 PMID: 24714687

36. Bhakdi S, Torzewski M, Klouche M, Hemmes M. Complement and atherogenesis binding of CRP to degraded, nonoxidized LDL enhances complement activation. Arteriosclerosis, thrombosis, and vascular biology. 1999; 19(10):2348–54. PMID: 10521363

37. Wieland E, Parthasarathy S, Steinberg D. Peroxidase-dependent metal-independent oxidation of low density lipoprotein in vitro: a model for in vivo oxidation? Proceedings of the National Academy of Sciences. 1993; 90(13):5929–33.

38. Ecker J, Langmann T, Moehle C, Schmitz G. Isomer specific effects of Conjugated Linoleic Acid on macrophage ABCG1 transcription by a SREBP-1c dependent mechanism. Biochemical and biophysical research communications. 2007; 352(3):805–11. doi: 10.1016/j.bbrc.2006.11.087 PMID: 17141191

39. Stöhr J, Schindler G, Rothe G, Schmitz G. Enhanced upregulation of the Fcγ receptor IIIa (CD16a) during in vitro differentiation of ApoE4/4 monocytes. Arteriosclerosis, thrombosis, and vascular biology. 1998; 18(9):1424–32. PMID: 9743231

40. Rogler G, Trümbach B, Klima B, Lackner KJ, Schmitz G. HDL-mediated efflux of intracellular cholesterol is impaired in fibroblasts from Tangier disease patients. Arteriosclerosis, thrombosis, and vascular biology. 1995; 15(5):683–90. PMID: 7749882

41. Bligh EG, Dyer WJ. A rapid method of total lipid extraction and purification. Canadian journal of biochemistry and physiology. 1959; 37(8):911–7. doi: 10.1139/o59-099 PMID: 13671378

42. Scherer M, Schmitz G, Liebisch G. High-throughput analysis of sphingosine 1-phosphate, sphinganine 1-phosphate, and lysophosphatidic acid in plasma samples by liquid chromatography—tandem mass spectrometry. Clinical chemistry. 2009; 55(6):1218–22. doi: 10.1373/clinchem.2008.113779 PMID: 19325012

43. Leidl K, Liebisch G, Richter D, Schmitz G. Mass spectrometric analysis of lipid species of human circulating blood cells. Biochimica et Biophysica Acta (BBA)-Molecular and Cell Biology of Lipids. 2008; 1781(10):655–64.

44. Scherer M, Leuthäuser-Jaschinski K, Ecker J, Schmitz G, Liebisch G. A rapid and quantitative LC-MS/MS method to profile sphingolipids. Journal of lipid research. 2010:jlr. D005322.

45. Liebisch G, Lieser B, Rathenberg J, Drobnik W, Schmitz G. High-throughput quantification of phosphatidylcholine and sphingomyelin by electrospray ionization tandem mass spectrometry coupled with isotope correction algorithm. Biochimica et Biophysica Acta (BBA)-Molecular and Cell Biology of Lipids. 2004; 1686(1):108–17.

46. Liebisch G, Drobnik W, Reil M, Trümbach B, Arnecke R, Olgemöller B, et al. Quantitative measurement of different ceramide species from crude cellular extracts by electrospray ionization tandem mass spectrometry (ESI-MS/MS). Journal of lipid research. 1999; 40(8):1539–46. PMID: 10428992

47. Liebisch G, Vizcaíno JA, Köfeler H, Trötzmüller M, Griffiths WJ, Schmitz G, et al. Shorthand notation for lipid structures derived from mass spectrometry. Journal of lipid research. 2013:jlr. M033506.

48. Herec M, Gagos M, Kulma M, Kwiatkowska K, Sobota A, Gruszecki WI. Secondary structure and orientation of the pore-forming toxin lysenin in a sphingomyelin-containing membrane. Biochim Biophys Acta. 2008; 1778(4):872–9. Epub 2008/01/08. doi: 10.1016/j.bbamem.2007.12.004 PMID: 18178147.

49. Buechler C, Bodzioch M, Bared SM, Sigruener A, Boettcher A, Lapicka-Bodzioch K, et al. Expression pattern and raft association of NIPSNAP3 and NIPSNAP4, highly homologous proteins encoded by genes in close proximity to the ATP-binding cassette transporter A1. Genomics. 2004; 83(6):1116–24. doi: 10.1016/j.ygeno.2003.12.011 PMID: 15177564

50. Sieber JJ, Willig KI, Heintzmann R, Hell SW, Lang T. The SNARE motif is essential for the formation of syntaxin clusters in the plasma membrane. Biophysical journal. 2006; 90(8):2843–51. doi: 10.1529/biophysj.105.079574 PMID: 16443657

51. Ecker J, Liebisch G, Englmaier M, Grandl M, Robenek H, Schmitz G. Induction of fatty acid synthesis is a key requirement for phagocytic differentiation of human monocytes. ProcNatlAcadSciUSA. 2010; 107 (17):7817–22.

52. Dhaliwal BS, Steinbrecher UP. Cholesterol delivered to macrophages by oxidized low density lipoprotein is sequestered in lysosomes and fails to efflux normally. Journal of lipid research. 2000; 41 (10):1658–65. PMID: 11013308

53. Kapinsky M, Torzewski M, Büchler C, Duong CQ, Rothe G, Schmitz G. Enzymatically degraded LDL preferentially binds to CD14high CD16+ monocytes and induces foam cell formation mediated only in part by the class B scavenger-receptor CD36. Arteriosclerosis, thrombosis, and vascular biology. 2001; 21(6):1004–10. PMID: 11397711

54. Li L, Sawamura T, Renier G. Glucose enhances human macrophage LOX-1 expression role for LOX-1 in glucose-induced macrophage foam cell formation. Circulation research. 2004; 94(7):892–901. doi: 10.1161/01.RES.0000124920.09738.26 PMID: 15001526

55. Asmis R, Begley JG. Oxidized LDL Promotes Peroxide-Mediated Mitochondrial Dysfunction and Cell Death in Human Macrophages A Caspase-3–Independent Pathway. Circulation research. 2003; 92(1): e20–e9. PMID: 12522131

56. Orsó E, Matysik S, Grandl M, Liebisch G, Schmitz G. Human native, enzymatically modified and oxidized low density lipoproteins show different lipidomic pattern. Biochimica et Biophysica Acta (BBA)-Molecular and Cell Biology of Lipids. 2015; 1851(3):299–306.

57. Kinscherf R, Claus R, Deigner HP, Nauen O, Gehrke C, Hermetter A, et al. Modified low density lipoprotein delivers substrate for ceramide formation and stimulates the sphingomyelin-ceramide pathway in human macrophages. FEBS letters. 1997; 405(1):55–9. PMID: 9094423

58. Miguet C, Monier S, Bettaieb A, Athias A, Bessede G, Laubriet A, et al. Ceramide generation occurring during 7b-hydroxycholesterol and 7-ketocholesterol-induced apoptosis is caspase independent and is not required to trigger cell death. Cell Death Differ. 2001; 8(1):83–99. doi: 10.1038/sj.cdd.4400792 PMID: 11313706

59. Nagy L, Tontonoz P, Alvarez JG, Chen H, Evans RM. Oxidized LDL regulates macrophage gene expression through ligand activation of PPARγ. Cell. 1998; 93(2):229–40. PMID: 9568715

60. Robbesyn F, Salvayre R, Negre-Salvayre A. Dual role of oxidized LDL on the NF-kappaB signaling pathway. Free radical research. 2004; 38(6):541–51. PMID: 15346645

61. Bhadra S, Arshad M, Rymaszewski Z, Norman E, Wherley R, Subbiah M. Oxidation of cholesterol moiety of low density lipoprotein in the presence of human endothelial cells or Cu+ 2 ions: identification of major products and their effects. Biochemical and biophysical research communications. 1991; 176 (1):431–40. PMID: 2018531

62. Gulbins E, Kolesnick R. Raft ceramide in molecular medicine. Oncogene. 2003; 22(45):7070–7. doi: 10. 1038/sj.onc.1207146 PMID: 14557812

63. Tam C, Idone V, Devlin C, Fernandes MC, Flannery A, He X, et al. Exocytosis of acid sphingomyelinase by wounded cells promotes endocytosis and plasma membrane repair. The Journal of cell biology. 2010; 189(6):1027–38. doi: 10.1083/jcb.201003053 PMID: 20530211

64. Rozenova KA, Deevska GM, Karakashian AA, Nikolova-Karakashian MN. Studies on the role of acid sphingomyelinase and ceramide in the regulation of tumor necrosis factor α (TNFα)-converting enzyme activity and TNFα secretion in macrophages. Journal of Biological Chemistry. 2010; 285(27):21103–13. doi: 10.1074/jbc.M109.080671 PMID: 20236926

65. Gulbins E, Li PL. Physiological and pathophysiological aspects of ceramide. American Journal of Physiology-Regulatory, Integrative and Comparative Physiology. 2006; 290(1):R11–R26. doi: 10.1152/ ajpregu.00416.2005 PMID: 16352856

66. London E. Ceramide Selectively Displaces Cholesterol from Ordered Lipid Domains (Rafts) Implications for lipid raft structure and function. Journal of Biological Chemistry. 2004; 279(11):9997–10004. doi: 10.1074/jbc.M309992200 PMID: 14699154

67. Bournazos S, Hart SP, Chamberlain LH, Glennie MJ, Dransfield I. Association of FcγRIIa (CD32a) with lipid rafts regulates ligand binding activity. The Journal of Immunology. 2009; 182(12):8026–36. doi: 10. 4049/jimmunol.0900107 PMID: 19494328

68. de la Haba C, Palacio JR, Martínez P, Morros A. Effect of oxidative stress on plasma membrane fluidity of THP-1 induced macrophages. Biochimica et Biophysica Acta (BBA)-Biomembranes. 2013; 1828 (2):357–64.

69. Myers SJ, Stanley KK. Src family kinase activation in glycosphingolipid-rich membrane domains of endothelial cells treated with oxidised low density lipoprotein. Atherosclerosis. 1999; 143(2):389–97. PMID: 10217369

70. Gaus K, Kritharides L, Schmitz G, Boettcher A, Drobnik W, Langmann T, et al. Apolipoprotein A-1 interaction with plasma membrane lipid rafts controls cholesterol export from macrophages. The FASEB journal. 2004; 18(3):574–6. doi: 10.1096/fj.03-0486fje PMID: 14734645

71. Fukuta S, Magnani JL, Twiddy EM, Holmes RK, Ginsburg V. Comparison of the carbohydrate-binding specificities of cholera toxin and Escherichia coli heat-labile enterotoxins LTh-I, LT-IIa, and LT-IIb. Infection and immunity. 1988; 56(7):1748–53. PMID: 3290106

72. Masserini M, Freire E, Palestini P, Calappi E, Tettamanti G. Fuc-GM1 ganglioside mimics the receptor function of GM1 for cholera toxin. Biochemistry. 1992; 31(8):2422–6. PMID: 1311601

73. Angström J, Teneberg S, Karlsson K-A. Delineation and comparison of ganglioside-binding epitopes for the toxins of Vibrio cholerae, Escherichia coli, and Clostridium tetani: evidence for overlapping epitopes. Proceedings of the National Academy of Sciences. 1994; 91(25):11859–63.

74. Kuziemko GM, Stroh M, Stevens RC. Cholera toxin binding affinity and specificity for gangliosides determined by surface plasmon resonance. Biochemistry. 1996; 35(20):6375–84. doi: 10.1021/bi952314i PMID: 8639583

75. Lauer S, Goldstein B, Nolan RL, Nolan JP. Analysis of cholera toxin-ganglioside interactions by flow cytometry. Biochemistry. 2002; 41(6):1742–51. PMID: 11827518

76. Drobnik W, Borsukova H, Böttcher A, Pfeiffer A, Liebisch G, Schütz GJ, et al. Apo AI/ABCA1-Dependent and HDL3-Mediated Lipid Efflux from Compositionally Distinct Cholesterol-Based Microdomains. Traffic. 2002; 3(4):268–78. PMID: 11929608

77. Witting SR, Maiorano JN, Davidson WS. Ceramide enhances cholesterol efflux to apolipoprotein AI by increasing the cell surface presence of ATP-binding cassette transporter A1. Journal of Biological Chemistry. 2003; 278(41):40121–7. doi: 10.1074/jbc.M305193200 PMID: 12890677

78. Luan Y, Griffiths HR. Ceramides reduce CD36 cell surface expression and oxidised LDL uptake by monocytes and macrophages. Archives of biochemistry and biophysics. 2006; 450(1):89–99. doi: 10.1016/j.abb.2006.03.016 PMID: 16620763

79. Sviridov D, Fidge N, Beaumier-Gallon G, Fielding C. Apolipoprotein AI stimulates the transport of intracellular cholesterol to cell-surface cholesterol-rich domains (caveolae). Biochemical Journal. 2001; 358 (Pt 1):79. PMID: 11485554

80. Zhu X, Owen JS, Wilson MD, Li H, Griffiths GL, Thomas MJ, et al. Macrophage ABCA1 reduces MyD88-dependent Toll-like receptor trafficking to lipid rafts by reduction of lipid raft cholesterol. Journal of lipid research. 2010; 51(11):3196–206. doi: 10.1194/jlr.M006486 PMID: 20650929

81. Fessler MB, Parks JS. Intracellular lipid flux and membrane microdomains as organizing principles in inflammatory cell signaling. The Journal of Immunology. 2011; 187(4):1529–35. doi: 10.4049/jimmunol.1100253 PMID: 21810617

82. van den Elzen P, Garg S, León L, Brigl M, Leadbetter EA, Gumperz JE, et al. Apolipoprotein-mediated pathways of lipid antigen presentation. Nature. 2005; 437(7060):906–10. doi: 10.1038/nature04001 PMID: 16208376